Flow Induced Vibration, Ziada & Staubli (eds) © 2000 Balkema, Rotterdam, ISBN 90 5809 129 5

An improved linear model for rotors subjected to dissipative annular flows

M. Moreira
Escola Superior de Technologia de Setúbal do IPS, Portugal

J. Antunes
Instituto Tecnológico e Nuclear, Sacavém, Portugal

H. Pina
Instituto Superior Técnico, Lisboa, Portugal

ABSTRACT: In a previous paper, Antunes, Axisa and co-workers developed a linearized model for the dynamic of rotors under moderate fluid confinement, based on classical perturbation analysis covering two different cases: (i) dissipative motions of a centered rotor; (ii) motions of an eccentric rotor for a frictionless flow. Following the same procedures and assumptions, we derive here an improved model to cover the more general case of a dissipative linearized motion of an eccentric rotor. Besides the natural position variables, a new flow variable, which can be physically interpreted as the fluctuating term of average tangential velocity, was introduced, yielding an additional eigenvalue in the linear analysis. The new variable introduced, coupled with the rotor motions, is unavoidable when frictional effects are not neglected and yield a richer modal behavior which can be related with delay effects of the flow responses to the abovementioned rotor motions. Because system dynamics are strongly dependent on actual rotor eccentricity, the validity of this model (or other linear model) is dependent on an adequate estimation of this parameter.

1 INTRODUCTION

In a previous paper, Antunes et al. (1996), developed a linearized model for the dynamic of rotors under moderate fluid confinement, based on classical perturbation analysis, covering two different cases:

1. Dissipative linearized motions of a centered rotor;
2. Linearized motions of an eccentric rotor for a frictionless flow.

This work showed, in particular, that system dynamics are quite sensitive to eccentricity and dissipative effects. Indeed, for moderate or high values of the rotor eccentricity, the system become unstable by divergence–at spinning velocities much lower than those for which the concentric rotors flutters. Quantitative differences in the dynamic behavior are controlled by the friction-dependent flow terms.

Following the same procedures and assumptions, we derive here an improved model to cover the more general case of a *dissipative linearized motion of an eccentric rotor*, whose study presents some further difficulties.

In this general situation, which was only previously covered in a crude way, the coupling between an auxiliary co-rotating flow variable and the rotor motions are introduced and yield an additional eigenvalue in the linear analysis.

2 FLOW FORMULATION

Consider the geometry of the fluid annulus represented in Figure 1, where θ and t are respectively the azimuth and time, R is the shaft radius and $u(\theta, t)$ is the gap-averaged tangential flow velocity. The annular gap depth $h(\theta, t)$ is very well approximated by

$$h(\theta,t) = H - (X_0 + X(t))\cos\theta - Y(t)\sin\theta \tag{1}$$

where H is the average annular gap and X_0 is some initial static eccentricity. Note that one can always choose an adequate orientation of coordinate axis to express the initial static eccentricity by X_0.

The following simplifying assumptions will be adopted concerning the flow field:

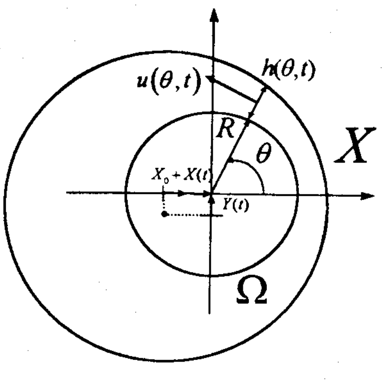

Figure 1: Geometry of the fluid annulus.

1. The flow is modeled as being two-dimensional and incompressible;
2. The radial gradients in the velocity and pressure fields are neglected;
3. The dissipative effects due to turbulent shear stresses at the walls are modeled using semiempirical loss-of-head terms.

Given the above assumptions one can obtain the continuity equation for incompressible flow and the momentum equation (projected in the tangential direction),

$$\frac{\partial h}{\partial t}+\frac{1}{R}\frac{\partial (hu)}{\partial \theta}=0, \qquad (2)$$

$$\rho\left\{\frac{\partial (hu)}{\partial t}+\frac{1}{R}\frac{\partial (hu^2)}{\partial \theta}\right\}+\tau_s+\tau_r+\frac{h}{R}\frac{\partial p}{\partial \theta}=0, \qquad (3)$$

where ρ is the fluid density and $p(\theta,t)$ is the gap-averaged pressure.

The shear stresses at the rotor and stator walls, in equation (3), are given by

$$\begin{cases} \tau_s(\theta,t)=\frac{1}{2}\rho u\,|u|\,f_s, \\ \tau_r(\theta,t)=-\frac{1}{2}\rho\,(\Omega R-u)\,|\Omega R-u|\,f_r, \end{cases} \qquad (4)$$

where f_r and f_s are empirical friction coefficients, which depend on the flow Reynolds number and on wall rugosity.

Assuming $f_r=f_s=f$ and adopting the simplifications discussed in Antunes et al. (1999), we can deduce

$$\tau_s+\tau_r\simeq \rho f\Omega R u-\frac{1}{2}\rho f\Omega^2R^2. \qquad (5)$$

Using classical perturbation analysis, equations (2) and (3), can be solved for a given motion of the rotor separating the displacement $h(\theta,t)$ the tangential flow velocity $u(\theta,t)$ and the pressure field $p(\theta,t)$ into a steady term, depending on the annulus eccentricity, and a small fluctuating term, dependent on the rotor vibratory motion

$$h(\theta,t) = h_0(\theta)+h_1(\theta,t), \qquad (6)$$

$$u(\theta,t) = u_0(\theta)+u_1(\theta,t), \qquad (7)$$

$$p(\theta,t) = p_0(\theta)+p_1(\theta,t). \qquad (8)$$

Replacing $h(\theta,t)$, $u(\theta,t)$ and $p(\theta,t)$ in (2), (3) and (5), by (6), (7) and (8), two sets of differential equations are obtained:

1. zero-order nonlinear flow equations, describing the steady flow field;
2. first-order linearized equations, describing the fluctuating flow, which apply to small vibratory motions about the static position.

In the following we will be interested, in particular, in the fluctuating linearized forms of the dynamic flow forces

$$\begin{cases} \frac{F_X(t)}{L}=-R\int_0^{2\pi}p_1(\theta,t)\cos\theta d\theta, \\ \frac{F_Y(t)}{L}=-R\int_0^{2\pi}p_1(\theta,t)\sin\theta d\theta, \end{cases} \qquad (9)$$

where L is the immersed length of the rotor. Equivalently, by an integration by parts, one can express equations (9) in a more convenient way as

$$\begin{cases} \frac{F_X(t)}{L}=R\int_0^{2\pi}\frac{\partial p_1(\theta,t)}{\partial\theta}\sin\theta d\theta, \\ \frac{F_Y(t)}{L}=-R\int_0^{2\pi}\frac{\partial p_1(\theta,t)}{\partial\theta}\cos\theta d\theta. \end{cases} \qquad (10)$$

3 SOLUTION OF THE FLOW EQUATIONS

3.1 *Analysis of the steady flow*

From the zero-order flow equations (see, Antunes et al. 1996) one can obtain the following steady parameters needed later to describe the fluctuating flow:

$$h_0(\theta)=H\,(1-\varepsilon\cos\theta), \qquad (11)$$

where $\varepsilon=\frac{X_0}{H}$ is the reduced initial static eccentricity,

$$u_0(\theta)=K\Omega R\frac{1}{1-\varepsilon\cos\theta}, \qquad (12)$$

with $K=\frac{1}{2}(1-\varepsilon^2)$ and finally,

$$\frac{\partial p_0(\theta)}{\partial\theta}=(\Omega R)^2\rho\left\{\begin{array}{l} A_1\frac{\partial F_2^{00}(\varepsilon,\theta)}{\partial\theta} \\ +A_2\frac{\partial F_2^{10}(\varepsilon,\theta)}{\partial\theta} \\ +A_3\frac{\partial F_2^{11}(\varepsilon,\theta)}{\partial\theta} \end{array}\right\} \qquad (13)$$

In the last equation,

$$A_1 = -\frac{1}{2}K^2, \qquad (14)$$

$$A_2 = -Kf\varepsilon\frac{1}{(1-\varepsilon^2)\,\delta}, \qquad (15)$$

$$A_3 = K\varepsilon^2 f\frac{1}{(1-\varepsilon^2)\,\delta} = -A_2\varepsilon, \qquad (16)$$

with $\delta = \frac{H}{R}$ and

$$F_k^{ij}(\varepsilon,\theta) = \frac{(\sin\theta)^i(\cos\theta)^j}{(1-\varepsilon\cos\theta)^k}. \qquad (17)$$

3.2 *Analysis of the fluctuating flow*

The linearized first-order equations are formulated as

$$\frac{\partial h_1}{\partial t} + \frac{1}{R}\frac{\partial}{\partial\theta}(h_0 u_1 + u_0 h_1) = 0, \qquad (18)$$

$$\begin{aligned} -\frac{\partial p_1}{\partial\theta} &= \tfrac{1}{h_0}\tfrac{\partial p_0}{\partial\theta}h_1 + R\rho\tfrac{u_0}{h_0}\tfrac{\partial h_1}{\partial t} + R\rho\tfrac{\partial u_1}{\partial t} \qquad (19)\\ &+2\rho\tfrac{u_0}{h_0}\tfrac{\partial h_0}{\partial\theta}u_1 + \rho\tfrac{u_0^2}{h_0}\tfrac{\partial h_1}{\partial\theta} + 2\rho\tfrac{\partial u_0}{\partial\theta}u_1\\ &+2\rho\tfrac{u_0}{h_0}\tfrac{\partial u_0}{\partial\theta}h_1 + 2\rho u_0\tfrac{\partial u_1}{\partial\theta} + \rho f\Omega R^2\tfrac{u_1}{h_0}, \end{aligned}$$

where

$$h_1 = -X\cos\theta - Y\sin\theta. \qquad (20)$$

From (11) and (12) one can solve (18) in order to obtain

$$\begin{aligned} u_1(\theta,t) &= \tfrac{K\Omega}{\delta}\tfrac{\cos\theta}{(1-\varepsilon\cos\theta)^2}X + \tfrac{K\Omega}{\delta}\tfrac{\sin\theta}{(1-\varepsilon\cos\theta)^2}Y\\ &+\tfrac{1}{\delta}\tfrac{\sin\theta}{(1-\varepsilon\cos\theta)}\dot{X} - \tfrac{1}{\delta}\tfrac{\cos\theta}{(1-\varepsilon\cos\theta)}\dot{Y}\\ &+\frac{C(t)}{(1-\varepsilon\cos\theta)} \qquad (21) \end{aligned}$$

where $C(t)$ is an integration "constant" related to the co-rotating flow.

3.3 *Resultant fluctuating fluid forces*

Considering equation (19), and with the knowledge of equations (11), (12), (13), (20) and, (21), one can deduce by integration,

$$\begin{aligned} f_X &\equiv \frac{F_X(t)}{L} = -R\int_0^{2\pi}\frac{\partial p_1(\theta,t)}{\partial\theta}\sin\theta d\theta \qquad (22)\\ &= \mathbf{M}_{XX}\ddot{X} + \mathbf{C}_{XX}\dot{X} + \mathbf{C}_{XY}\dot{Y}\\ &+\mathbf{K}_{XX}X + \mathbf{K}_{XY}Y + \mathbf{K}_{XC}C, \end{aligned}$$

$$\begin{aligned} f_Y &\equiv \frac{F_Y(t)}{L} = R\int_0^{2\pi}\frac{\partial p_1(\theta,t)}{\partial\theta}\cos\theta d\theta \qquad (23)\\ &= \mathbf{M}_{YY}\ddot{Y} + \mathbf{C}_{YX}\dot{X} + \mathbf{C}_{YY}\dot{Y} + \mathbf{C}_{YC}\dot{C}\\ &+\mathbf{K}_{YX}X + \mathbf{K}_{YY}Y + \mathbf{K}_{YC}C, \end{aligned}$$

$$\begin{aligned} f_C &\equiv R\int_0^{2\pi}\frac{\partial p_1(\theta,t)}{\partial\theta}d\theta = 0 \qquad (24)\\ &= \mathbf{M}_{CY}\ddot{Y} + \mathbf{C}_{CX}\dot{X} + \mathbf{C}_{CY}\dot{Y} + \mathbf{C}_{CC}\dot{C}\\ &+\mathbf{K}_{CX}X + \mathbf{K}_{CY}Y + \mathbf{K}_{CC}C. \end{aligned}$$

The inertial, velocity and displacement coupling factors are presented in Appendix A as a function of

$$G_k^{ij}(\varepsilon) = \int_0^{2\pi}\frac{(\sin\theta)^i(\cos\theta)^j}{(1-\varepsilon\cos\theta)^k}d\theta, \qquad (25)$$

which are tabled in Appendix B.

Observe that the dynamic of the system depends on $X(t)$, $Y(t)$ and $C(t)$. This explains why we need three equations (22), (23) and (24) to characterize f_X and f_Y which are the focus of our interest. However, in two particular cases (see, Antunes et al. 1996) it is possible to characterize f_X and f_Y with only two equations: (i) dissipative linearized motions of a centered rotor; (ii) linearized motions of an eccentric rotor for a frictionless flow. In these situations one can eliminate references to the variable $C(t)$ and its derivative in equations (22) and (23).

3.4 *Physical meaning of* $C(t)$

Integrating each member of the linearized form of the flow rate

$$\begin{aligned} \Phi(t) &= h_0(\theta)\,u_0(\theta) \qquad (26)\\ &+h_1(\theta,t)\,u_0(\theta) + h_0(\theta)\,u_1(\theta,t), \end{aligned}$$

in $[0,2\pi]$, one can obtain

$$\Phi(t) = HK\Omega R + HC(t)$$

that is,

$$\bar{u}(t) = C_0 + C(t)$$

where $\bar{u}(t) = \frac{\Phi(t)}{H}$ is the average tangential flow velocity and $C_0 = K\Omega R$ is the correspondent zero order term. Clearly, $C(t)$ is the first order fluctuating term of the average tangential flow velocity.

4 ANALYSIS OF THE COUPLED SYSTEM

4.1 *Adopted formalism*

Let f_X^{st} and f_Y^{st} be the structural forces per unit length

$$f_X^{st} = M^{st}\ddot{X} + C^{st}\dot{X} + K^{st}X, \qquad (27)$$

$$f_Y^{st} = M^{st}\ddot{Y} + C^{st}\dot{Y} + K^{st}Y, \qquad (28)$$

where and M^{st}, C^{st} and K^{st} stand respectively for the simple rigid rotor mass, the flexible isotropic rotor fixture and the corresponding stiffness, per unit length. The study of the phenomena induced by the co-rotating flow can be made considering the following complete set of rotodynamic equations

$$\begin{aligned} f_X + f_X^{st} &= (\mathbf{M}_{XX} + M^{st})\ddot{X} \\ &+ (\mathbf{C}_{XX} + C^{st})\dot{X} + \mathbf{C}_{XY}\dot{Y} \\ &+ (\mathbf{K}_{XX} + K^{st})X + \mathbf{K}_{XY}Y + \mathbf{K}_{XC}C, \end{aligned} \qquad (29)$$

$$\begin{aligned} f_Y + f_Y^{st} &= (\mathbf{M}_{YY} + M^{st})\ddot{Y} + \mathbf{C}_{YX}\dot{X} \\ &+ (\mathbf{C}_{YY} + C^{st})\dot{Y} + \mathbf{C}_{YC}\dot{C} \\ &+ \mathbf{K}_{YX}X + (\mathbf{K}_{YY} + K^{st})Y + \mathbf{K}_{YC}C, \end{aligned} \qquad (30)$$

$$\begin{aligned} 0 &= \mathbf{M}_{CY}\ddot{Y} + \mathbf{C}_{CX}\dot{X} \\ &+ \mathbf{C}_{CY}\dot{Y} + \mathbf{C}_{CC}\dot{C} \\ &+ \mathbf{K}_{CX}X + \mathbf{K}_{CY}Y + \mathbf{K}_{CC}C. \end{aligned} \qquad (31)$$

Letting $Z = \dot{X}$ and $W = \dot{Y}$ one can study the modal behavior of the system as a function of ε and Ω, solving the complex eigenvalue $\lambda_n = \sigma_n + i\nu_n$ and complex eigenvector $\{\Phi_n\}$ problems, of an equivalent set of five first order differential equations.

From each eigenvalue $\lambda_n = \sigma_n + i\nu_n$, the corresponding reduced modal frequency and reduced modal damping can be computed as $\varpi_n = \frac{\nu_n}{\omega^{st}}$ and $\bar{d}_n = \frac{-\sigma_n}{\omega^{st}}$, where ω^{st} is the structural ***in vacuum*** radian frequency.

0, 1 or 2 complex conjugate pairs of eigenvalues (and eigenvectors) would be expected in the complete set of 5 eigenvalues (and eigenvectors) of the problem. Observe that one of the eigenvalues must be always real.

4.2 *Alternative formalism*

Note that in the preceding analysis we deal with a new variable, $C(t)$. However, admitting a solution in the form

$$\bar{S} = \begin{bmatrix} X_0 \\ Y_0 \\ C_0 \end{bmatrix} e^{\lambda t},$$

and substituting it in the homogeneous form of equations (29), (30) and (31) one can deduce after eliminating C_0

$$\{\lambda^2\mathbf{M} + \lambda\mathbf{C} + \mathbf{K}\}\begin{bmatrix} X_0 \\ Y_0 \end{bmatrix} = \begin{bmatrix} 0 \\ 0 \end{bmatrix} \qquad (32)$$

where

$$\mathbf{M} = \begin{bmatrix} \mathbf{M}_{XX} + M^{st} & \frac{-\mathbf{M}_{CY}\mathbf{K}_{XC}}{D} \\ \frac{-\mathbf{C}_{YC}\mathbf{C}_{CX}}{D} & \begin{matrix} \mathbf{M}_{YY} + M^{st} \\ -\frac{\mathbf{K}_{YC}\mathbf{M}_{CY} + \mathbf{C}_{YC}\mathbf{C}_{CY}}{D} \\ -\lambda\frac{\mathbf{C}_{YC}\mathbf{M}_{CY}}{D} \end{matrix} \end{bmatrix},$$

$$\mathbf{C} = \begin{bmatrix} \begin{matrix} \mathbf{C}_{XX} + C^{st} \\ -\frac{\mathbf{C}_{CX}\mathbf{K}_{XC}}{D} \end{matrix} & \begin{matrix} \mathbf{C}_{XY} \\ -\frac{\mathbf{C}_{CY}\mathbf{K}_{XC}}{D} \end{matrix} \\ \begin{matrix} \mathbf{C}_{YX} \\ -\frac{\mathbf{K}_{YC}\mathbf{C}_{CX} + \mathbf{C}_{YC}\mathbf{K}_{CX}}{D} \end{matrix} & \begin{matrix} \mathbf{C}_{YY} + C^{st} \\ -\frac{\mathbf{C}_{YC}\mathbf{K}_{CY} + \mathbf{K}_{YC}\mathbf{C}_{CY}}{D} \end{matrix} \end{bmatrix};$$

$$\mathbf{K} = \begin{bmatrix} \begin{matrix} \mathbf{K}_{XX} + K^{st} \\ -\frac{\mathbf{K}_{CX}\mathbf{K}_{XC}}{D} \end{matrix} & \begin{matrix} \mathbf{K}_{XY} \\ -\frac{\mathbf{K}_{CY}\mathbf{K}_{XC}}{D} \end{matrix} \\ \begin{matrix} \mathbf{K}_{YX} \\ -\frac{\mathbf{K}_{YC}\mathbf{K}_{CX}}{D} \end{matrix} & \begin{matrix} \mathbf{K}_{YY} + K^{st} \\ -\frac{\mathbf{K}_{YC}\mathbf{K}_{CY}}{D} \end{matrix} \end{bmatrix},$$

and $D = \lambda\mathbf{C}_{CC} + \mathbf{K}_{CC}$.

Observe that all the three matrices obtained, **M**, **C** and **K**, depend on the λ. Thus to solve the new generalized eigenvalue problem (32), and find the modal properties of the system, it is necessary to apply an iterative method.

This dependence can be interpreted as a delay in the response of the dynamic system to an excitation, in comparison to the correspondent response if the flow were non-dissipative, as can be found in a similar context in Porcher (1994).

As a matter of fact, if the flow is non-dissipative ($f = 0$) the matrices in equation (32) can be made independent of λ. In this case (if the flow is non-dissipative), one can deduce

$$\{\lambda^3\mathbf{N}_1 + \lambda^2\mathbf{N}_2 + \lambda\mathbf{N}_3 + \mathbf{N}_4\}\begin{bmatrix} X_0 \\ Y_0 \end{bmatrix} = \begin{bmatrix} 0 \\ 0 \end{bmatrix} \qquad (33)$$

where

$$\mathbf{N}_1 = \begin{bmatrix} (\mathbf{M}_{XX} + M^{st}) & 0 \\ 0 & \begin{matrix} (\mathbf{M}_{YY} + M^{st}) \\ -\frac{\mathbf{C}_{YC}\mathbf{M}_{CY}}{\mathbf{C}_{CC}} \end{matrix} \end{bmatrix},$$

$$\mathbf{N}_2 = \begin{bmatrix} (\mathbf{C}_{XX} + C^{st}) & \mathbf{C}_{XY} - \frac{\mathbf{M}_{CY}\mathbf{K}_{XC}}{\mathbf{C}_{CC}} \\ \mathbf{C}_{YX} - \frac{\mathbf{C}_{YC}\mathbf{C}_{CX}}{\mathbf{C}_{CC}} & (\mathbf{C}_{YY} + C^{st}) \end{bmatrix},$$

$$\mathbf{N}_3 = \begin{bmatrix} (\mathbf{K}_{XX} + K^{st}) - \frac{\mathbf{C}_{CX}\mathbf{K}_{XC}}{\mathbf{C}_{CC}} & 0 \\ 0 & (\mathbf{K}_{YY} + K^{st}) - \frac{\mathbf{C}_{YC}\mathbf{K}_{CY}}{\mathbf{C}_{CC}} \end{bmatrix},$$

and

$$\mathbf{N}_4 = \begin{bmatrix} 0 & -\frac{\mathbf{K}_{CY}\mathbf{K}_{XC}}{\mathbf{C}_{CC}} \\ 0 & 0 \end{bmatrix}.$$

To justify that the response of the dissipative system [equation (32)] is delayed in comparison to the response of the non-dissipative system [equation (33)], one can briefly study the simpler analogous planar case.

1) Dissipative planar case

Letting $Y = \dot{Y} = \ddot{Y} = 0$, the homogeneous form of equations (29), (30) and (31) collapse into the following system of two independent differential equations

$$\begin{aligned} 0 &= (\mathbf{M}_{XX} + M^{st})\ddot{X} + (\mathbf{C}_{XX} + C^{st})\dot{X} \\ &\quad + (\mathbf{K}_{XX} + K^{st})X + \mathbf{K}_{XC}C \end{aligned} \quad (34)$$

$$\begin{aligned} 0 &= \mathbf{C}_{CX}\dot{X} + \mathbf{C}_{CC}\dot{C} \\ &\quad + \mathbf{K}_{CX}X + \mathbf{K}_{CC}C. \end{aligned} \quad (35)$$

Exciting the dynamic system correspondent to equations (34) and (35) with $F = F_0 e^{\lambda_F t}$, where λ_F stands for a complex number, we obtain

$$\begin{aligned} F_0 e^{\lambda_F t} &= (\mathbf{M}_{XX} + M^{st})\ddot{X} + \\ &\quad + (\mathbf{C}_{XX} + C^{st})\dot{X} \\ &\quad + (\mathbf{K}_{XX} + K^{st})X + \mathbf{K}_{XC}C \end{aligned} \quad (36)$$

where

$$C(t) = -e^{-\frac{\mathbf{K}_{CC}}{\mathbf{C}_{CC}}t} \int \frac{e^{\frac{\mathbf{K}_{CC}}{\mathbf{C}_{CC}}t}\left(\mathbf{C}_{CX}\dot{X} + \mathbf{K}_{CX}X\right)}{\mathbf{C}_{CC}} dt. \quad (37)$$

After some manipulation, one can deduce the forced solution of equation (36)

$$X_{\text{dissapative}}(t) = \quad (38)$$

$$= \frac{(d + \zeta)e^{\lambda_F t}}{(a\lambda_F^3 + b\lambda_F^2 + c\lambda_F) + \alpha\lambda_F^2 + \beta\lambda_F + \eta}$$

where

$$\begin{aligned} a &= (\mathbf{M}_{XX} + M^{st}), \\ b &= (\mathbf{C}_{XX} + C^{st}), \\ c &= \left[(\mathbf{K}_{XX} + K^{st}) - \frac{\mathbf{K}_{XC}\mathbf{C}_{CX}}{\mathbf{C}_{CC}}\right], \\ d &= F_0\lambda_F, \\ \alpha &= (\mathbf{M}_{XX} + M^{st})\frac{\mathbf{K}_{CC}}{\mathbf{C}_{CC}}, \\ \beta &= \frac{(\mathbf{C}_{XX} + C^{st})\mathbf{K}_{CC}}{\mathbf{C}_{CC}}, \\ \eta &= \left[(\mathbf{K}_{XX} + K^{st})\frac{\mathbf{K}_{CC}}{\mathbf{C}_{CC}} - \frac{\mathbf{K}_{XC}\mathbf{K}_{CX}}{\mathbf{C}_{CC}}\right], \\ \zeta &= F_0\frac{\mathbf{K}_{CC}}{\mathbf{C}_{CC}}. \end{aligned}$$

2) Non-dissipative planar case

If $f = 0$, then $\mathbf{K}_{CX} = \mathbf{K}_{CC} = 0$ and the solution (38), can be simplified into

$$X_{\text{nondissipative}}(t) = \frac{d}{(a\lambda_F^3 + b\lambda_F^2 + c\lambda_F)}e^{\lambda_F t}. \quad (39)$$

One can identify a delay ϕ between responses (38) and (39) which we can compute as

$$\begin{aligned} \phi &= \arg\left(\frac{X_{\text{nondissipative}}(t)}{X_{\text{dissipative}}(t)}\right) \\ &= \arg\left(1 + \frac{(\alpha\lambda_F^2 + \beta\lambda_F + \eta)}{(a\lambda_F^3 + b\lambda_F^2 + c\lambda_F)}\right). \end{aligned}$$

Observe that α, β and η are zero, whenever $f = 0$.

5 NUMERICAL APPLICATIONS

As mentioned before in the eigenvalue analysis of the system correspondent to the differential equations from (29) to (31), we would expect to find 0, 1 or 2 complex conjugate pairs of eigenvalues (and eigenvectors) of the problem. This means that 5, 3 or 1 of the complete set of 5 eigenvalues will be real, respectively. Therefore, numerical results presented here do account for this fact.

Observe that each conjugate pair of complex eigenvalues/eigenvectors forms a *mode* as do each unpaired of the remaining real eigenvalues/eigenvectors. These modes can be represented by the corresponding frequency (imaginary part of the eigenvalue) and damping (real part of the same eigenvalue) which depend on spinning velocity. Zero different frequency modes can be additionally characterized by a well defined *forward* or *backward whirl*. The computed modes are identified in the plots using the following codes: F and B, respectively, for the forward and backward whirling modes and Z for the zero-frequency mode.

The reduced modal frequencies $\varpi_n = \frac{\nu_n}{\omega^{st}}$ are shown as a function of the reduced rotor velocity $\bar{\Omega} = \frac{\Omega}{\omega^{st}}$, as well the corresponding damping coefficient $\bar{d}_n = \frac{-\sigma_n}{\omega^{st}}$.

In order to be able to compare present results with previous work (Antunes et al. 1996), we have assumed a mass ratio $\gamma = \frac{M_a}{M_{st}} = 2$, a reduced gap of $\delta = H/R = 0.1$ and we have neglected all dissipative structural effects in all numerical simulations except the one in which we use an estimate of the actual eccentricity at each spinning velocity.

5.1 *Some cases accounted for by previous theory*

In Figures 2 to 5 we present some particular cases which have in common the fact they are *dissipative linearized motions of a centered rotor* or *linearized motions of an eccentric rotor for a frictionless flow*. That is, those cases are completely accounted for by the previous linear theory developed in Antunes et al. (1996).

In fact, the numerical results presented in these figures show the same forward and backward whirling modes represented in Figure 11 in Antunes et al. (1996) and, of course, one additionally new real mode (a zero frequency mode).

5.2 *The dissipative-eccentric case*

In Figure 6 the more general case of a *dissipative linearized motion of an eccentric rotor* is considered.

The numerical results presented are strongly different from the analogous numerical results computed in Antunes et al. (1996), and shown here in Figure 7. At that time this case was only treated in a crude way and the analysis was made under a natural superposition assumption performed over the developed linearized models.

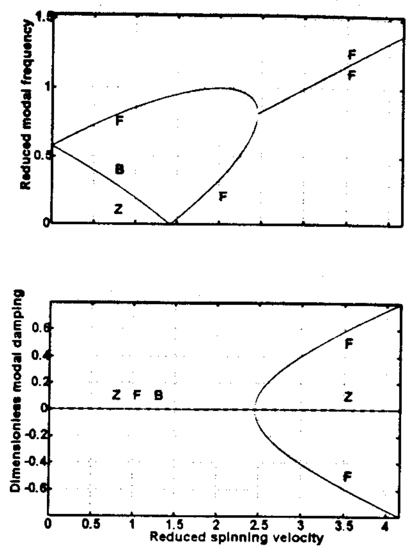

Figure 2: Rotor modes as a function of the reduced spinning velocity $\bar{\Omega}$ (rotor eccentricity $\varepsilon = 0$; fluid friction neglected; mass ratio $\gamma = 2$).

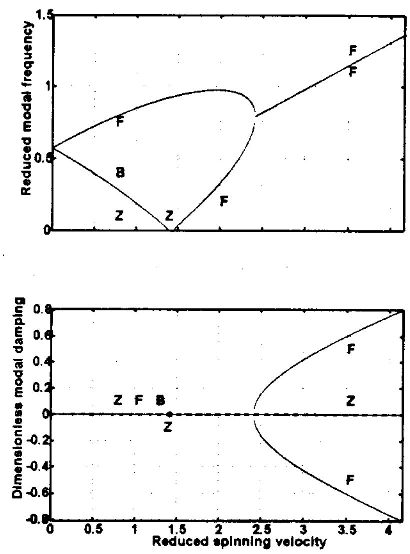

Figure 3: Rotor modes as a function of the reduced spinning velocity $\bar{\Omega}$ (rotor eccentricity $\varepsilon = 0.3$; fluid friction neglected; mass ratio $\gamma = 2$)

Comparing Figures 6 and 7 we can observe that the modal damping predicted by the new linear model exhibits significant differences which stress the importance of the new improved model.

One can note, for example, that in this configuration the improved linear model predicts that the system will become unstable, due to flutter, at a very early stage.

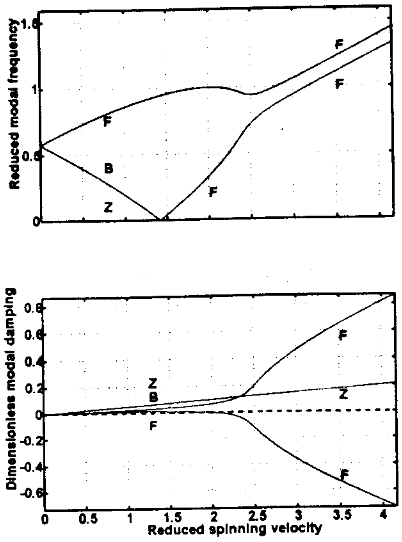

Figure 4: Rotor modes as a function of the reduced spinning velocity $\bar{\Omega}$ (rotor eccentricity $\varepsilon = 0$; fluid friction $f = 0.005$; mass ratio $\gamma = 2$).

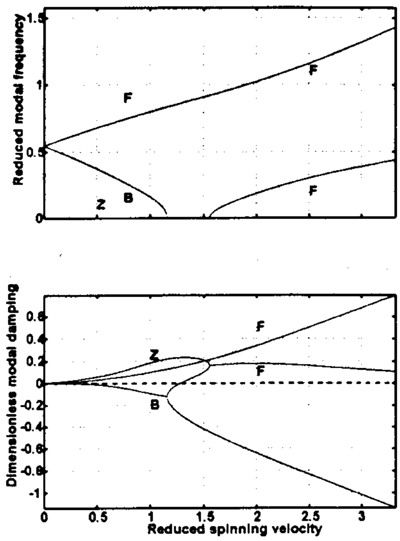

Figure 6: Rotor modes as a function of the reduced spinning velocity $\bar{\Omega}$ (rotor eccentricity $\varepsilon = 0.7$; fluid friction $f = 0.005$; mass ratio $\gamma = 2$).

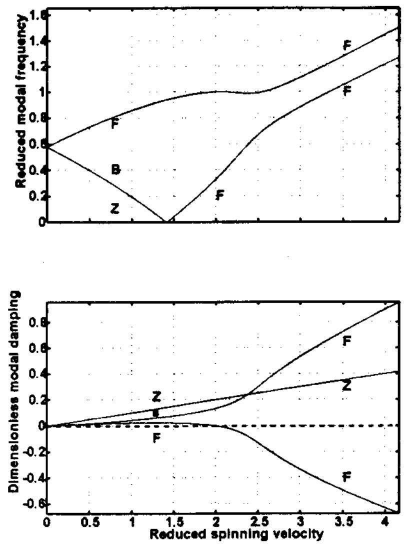

Figure 5: Rotor modes as a function of the reduced spinning velocity $\bar{\Omega}$ (rotor eccentricity $\varepsilon = 0$; fluid friction $f = 0.01$; mass ratio $\gamma = 2$).

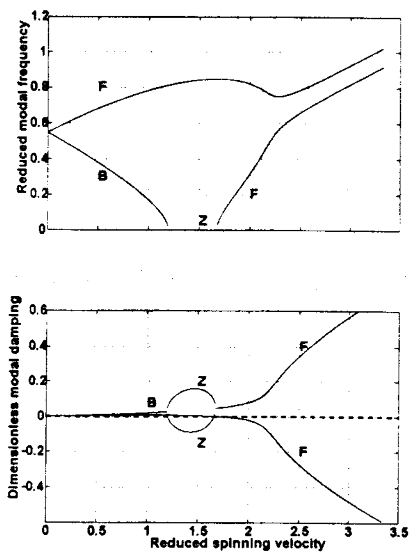

Figure 7: Rotor modes as a function of the reduced spinning velocity $\bar{\Omega}$ (rotor eccentricity $\varepsilon = 0.7$; fluid friction $f = 0.005$; mass ratio $\gamma = 2$).

5.3 *Using the actual eccentricity*

Numerical applications shown in this subsection are based on the experiments (using water) performed by Grunenwald et al. (1996) and in correspondent nonlinear simulations (Moreira et al. 2000a). In experiments and in nonlinear simulations this configuration was labeled "eccentric configuration B". The significant parameters used were tabled in these papers. Dissipative structural effects were now considered and the modal frequency and damping, presented, are not in a reduced form.

System dynamics are strongly dependent on rotor eccentricity. Moreover, the developed linear theory based on first-order linearized equations, describing the fluctuating flow, only applies to small vibratory motions about the static position of the rotor. Those facts, in the presence of a significant rotor drift (mostly due to a Bernoulli effect) as a function of the spinning velocity (see for instance, Grunenwald et al. 1996), motivate the usage of the *actual eccentricity* (or, at least, an estimate of it) in the eigenvalue analysis.

In Figures 8 and 9 one can see respectively the eigenvalue analysis using the same initial static eccentricity (for each spinning velocity) and an estimate of the drift. The actual eccentricity for each spinning velocity was estimated using a spline curve linking nonlinear numerical results of eccentricity at certain regimes which are displayed in Figure 10.

Differences exhibited justify this approach. Unfortunately there is no way to easily obtain an estimate of the drift.

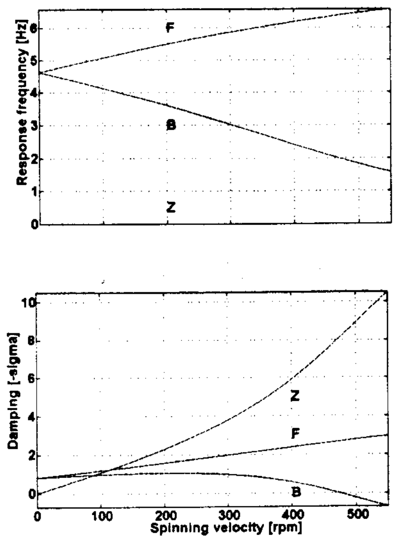

Figure 8: Rotor modes as a function of the spinning velocity using the same static eccentricity at each spinning velocity ($\varepsilon = 0.6$,"*eccentric configuration* B" in Grunenwald et al. 1996 & Moreira et al. 2000a).

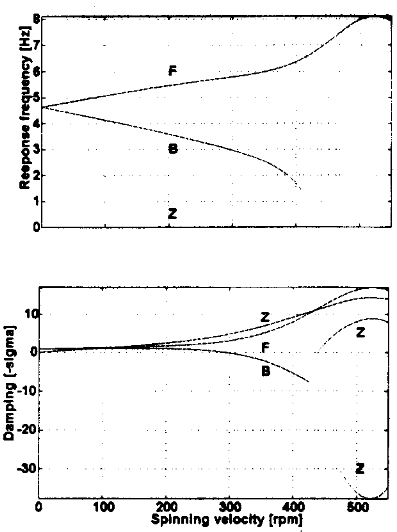

Figure 9: Rotor modes as a function of the spinning velocity using an estimate of the actual eccentricity ("*eccentric configuration* B" in Grunenwald et al. 1996 & Moreira et al. 2000a).

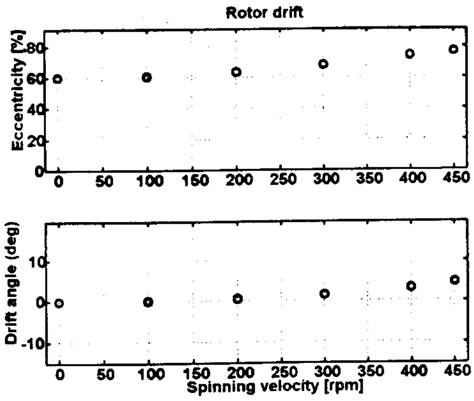

Figure 10: Nonlinear estimations of the rotor drift ("*eccentric configuration* B" in Moreira et al. 2000a).

6 CONCLUSIONS

In this paper an improved linear model for rotors subjected to dissipative annular flows based on classical perturbation analysis was developed.

Besides the natural position variables $X = X(t)$ and $Y = Y(t)$ of the problem, a new flow variable $C = C(t)$, which can be physically interpreted as the fluctuating term of average tangential velocity, was introduced, yielding an additional eigenvalue in the linear analysis (whenever boundary pressure values are controlled by dissipative effects an additional flow variable have to be introduced).

This model is an extension of the one developed in Antunes et al. (1996) and shows identical predictions in cases completely accounted for by the old one, namely: *(i) dissipative linearized motions of a centered rotor; (ii) linearized motions of an eccentric rotor for a frictionless flow*. However, the new model can also deal with *dissipative motions of eccentric rotors*.

The new variable introduced $C = C(t)$, coupled with $X = X(t)$ and $Y = Y(t)$, is unavoidable when frictional effects are not neglected and yield a richer modal behavior which can be related with delay effects of the flow responses to rotor motions.

Because system dynamics are strongly dependent on actual rotor eccentricity, the validity of this model (or other linear model) is dependent on an adequate estimation of this parameter.

Experimental work is currently being prepared to further assert the validity of the present linear model (Moreira et al. 2000b).

REFERENCES

Antunes, J., Axisa, F. & T. Grunenwald 1996. Dynamics of Rotors Immersed in Eccentric Annular Flow: Part 1 - Theory. *Journal of Fluids and Structures* 10: 893-918.

Antunes, J., Mendes, J., Moreira, M. & T. Grunenwald 1999. A Theoretical Model for Nonlinear Planar Motions of Rotors under Fluid Confinement. *Journal of Fluids and Structures* 13: 103-106.

Axisa, F. & J. Antunes 1992. Flexural Vibrations of Rotors Immersed in Dense Fluids: Part 1 - Theory. *Journal of Fluids and Structures* 6: 3-21.

Grunenwald, T., Axisa, F. & J. Antunes 1991. Rotor Vibration under Fluid Confinement: Analysis of Dissipative Phenomena and Stability. *Journal of Fluids and Structures* 10: 919-944.

T. Grunenwald 1994. Comportement Vibratoire d' Arbres de Machines Tournantes dans un Espace Annulaire de Fluide de Confinement Modéré. Doctoral Thesis, Paris University, September 1994.

Grunenwald, T., Axisa, F., Bennett, G. & J. Antunes 1996. Dynamics of Rotors Immersed in Eccentric Annular Flow: Part 2 - Experiments, *Journal of Fluids and Structures* 10: 919-944.

Moreira, M., Antunes, J., & H. Pina 2000a. A Theoretical Model for Nonlinear Orbital Motions of Rotors under Fluid Confinement. *Accepted for publication in Journal of Fluids and Structures.*

Moreira, M., Tissot, A. & J. Antunes 2000b. Experimental Validation of Theoretical Models for the Linear and Nonlinear Vibrations of Immersed Rotors. *Accepted for presentation in* ISROMAC-*8 (8*th International. Symposium on Transport Phenomena and Dynamics of Rotating Machinery), March 26-30, 2000.

M. G. Porcher 1994. Contribution à l'étude des instabilités fluide-élastiques de structures tubulaires, sous ecoulemen axial confinè, PhD Thesis presented at University of Paris 6.

NOMENCLATURE

$C(t)$	new flow variable.
C^{st}	structural damping per unit length.
$\bar{d}_n$	reduced modal damping $\bar{d}_n = \frac{-\sigma_n}{\omega^{st}}$.
f, f_r, f_s	friction coefficients.
f^{st}	structural *in vacuo* frequency.
f_X, f_Y, f_C	fluidelastic forces per unit length.
f_X^{st}, f_Y^{st}	structural forces per unit length.
$h(\theta,t)$	local gap.
h_0, h_1	steady and fluctuating local gap.
H	average annular gap.
K^{st}	structural stiffness per unit length.
L	rotor length.
M_a	added mass per unit length, $M_a = \frac{\pi R^2 \rho}{\delta}$
M^{st}	modal mass (with no fluid) per unit length.
$p(\theta,t)$	gap averaged pressure.
p_0, p_1	steady and fluctuating gap averaged presure.
R	rotor radius.
t	time.
$u(\theta,t)$	tangencial flow velocity.
u_0, u_1	steady and fluctuating tangencial flow velocity.
$X(t), Y(t)$	rotor motions.
X_0, Y_0	steady rotor positions.
γ	mass ratio, $\gamma = \frac{M_a}{M^{st}}$
δ	reduced gap: H/R.
ε	reduced initial static eccentricity, $\varepsilon = \frac{X_0}{H}$.
λ_n	eigenvalue of the flow-structure system.
θ	azimuthal angle.
ν_n	imaginary part of the eigenvalue λ_n.
ρ	fluid density.
σ_n	real part of the eigenvalue λ_n.
τ_r, τ_s	shear stresses at the rotor and stator walls.
ω_n	circular frequency.
ϖ_n	reduced modal frequency, $\varpi_n = \frac{\nu_n}{\omega^{st}}$
ω^{st}	structural *in vacum* radian frequency.
ϕ	delay.
Ω	spinning velocity.
$\bar{\Omega}$	reduced rotor velocity $\bar{\Omega} = \frac{\Omega}{\omega^{st}}$.

APPENDIX A: COUPLING FACTORS

$$\mathbf{M}_{XX} = R^2\rho\tfrac{1}{\delta}G_1^{20} \tag{A1}$$

$$\mathbf{M}_{XX} = R^2\rho\tfrac{1}{\delta}G_1^{20} \tag{A2}$$

$$\mathbf{M}_{XX} = R^2\rho\tfrac{1}{\delta}G_1^{20} \tag{A3}$$

$$\mathbf{C}_{XX} = \tfrac{\rho R^2}{\delta}\tfrac{f\Omega}{\delta}G_2^{20} \tag{A4}$$

$$\mathbf{C}_{XY} = \tfrac{R^2\rho}{\delta}2K\Omega G_3^{20} \tag{A5}$$

$$\mathbf{K}_{XX} = \tfrac{R^2\rho}{\delta}K^2\Omega^2\left(G_3^{20} - 2G_4^{20} - \varepsilon G_4^{21}\right) \tag{A6}$$

$$\mathbf{K}_{XY} = \tfrac{R^2\rho}{\delta}\tfrac{fK\Omega^2}{\delta}\begin{pmatrix} -\frac{\varepsilon^2}{(1-\varepsilon^2)}\left(G_4^{20} + G_4^{22}\right) \\ +\frac{\varepsilon\left(1+\varepsilon^2\right)}{(1-\varepsilon^2)}G_4^{21} + G_3^{20} \end{pmatrix} \tag{A8}$$

$$\mathbf{K}_{XC} = -2\rho K\Omega R^2\varepsilon G_3^{20} \tag{A9}$$

$$\mathbf{M}_{YY} = +\tfrac{R^2\rho}{\delta}G_1^{02} \tag{A10}$$

$$\mathbf{C}_{YY} = +\tfrac{R^2\rho}{\delta}\tfrac{f\Omega}{\delta}G_2^{02} \tag{A11}$$

$$\mathbf{C}_{YX} = +\tfrac{2\rho K\Omega R^2}{\delta}\left(-G_3^{02} + \varepsilon G_3^{01}\right) \tag{A12}$$

$$\mathbf{C}_{YC} = -R^2\rho G_1^{01} \tag{A13}$$

$$\mathbf{K}_{YX} = \tfrac{R^2\rho}{\delta}f\tfrac{\Omega^2}{\delta}K\begin{pmatrix} \frac{\varepsilon^2}{(1-\varepsilon^2)}\left(G_4^{02} + G_4^{04}\right) \\ -\left(\varepsilon G_4^{03} + G_3^{02}\right) \end{pmatrix} \tag{A14}$$

$$\mathbf{K}_{YY} = \tfrac{R^2\rho}{\delta}\Omega^2K^2\begin{pmatrix} -\varepsilon G_4^{21} + G_3^{02} - 2G_4^{02} \\ -\varepsilon 2G_4^{03} + 4\varepsilon G_4^{01} \end{pmatrix} \tag{A15}$$

$$\mathbf{K}_{YC} = -\tfrac{R^2\rho}{\delta}f\Omega G_2^{01} \tag{A16}$$

$$\mathbf{M}_{CY} = \tfrac{R^2\rho}{\delta}G_1^{01} \tag{A17}$$

$$\mathbf{C}_{CC} = -R^2\rho G_1^{00} \tag{A18}$$

$$\mathbf{C}_{CX} = \tfrac{R^2\rho}{\delta}2K\Omega\left(-G_3^{01} + \varepsilon G_3^{00}\right) \tag{A19}$$

$$\mathbf{C}_{CY} = \tfrac{f\Omega}{\delta}\tfrac{R^2\rho}{\delta}G_2^{01} \tag{A20}$$

$$\mathbf{K}_{CX} = \tfrac{R^2\rho}{\delta}\Omega^2\begin{pmatrix} -A_2\varepsilon\left(G_4^{01} + G_4^{03}\right) \\ +\left(1+\varepsilon^2\right)A_2G_4^{02} \\ -f\frac{K}{\delta}G_3^{01} \end{pmatrix} \tag{A21}$$

$$\mathbf{K}_{CX} = -\tfrac{R^2\rho}{\delta}\Omega^2\left(2f\tfrac{K}{\delta}\varepsilon\tfrac{\pi}{\sqrt{(1-\varepsilon^2)^5}}\right) \tag{A22}$$

$$\mathbf{K}_{CY} = \tfrac{R^2\rho}{\delta}K^2\Omega^2\begin{pmatrix} -\varepsilon G_4^{20} + G_3^{01} - 2G_4^{01} \\ -2\varepsilon G_4^{02} + 4\varepsilon G_4^{00} \end{pmatrix} \tag{A23}$$

$$\mathbf{K}_{CC} = -\tfrac{\rho f\Omega R^2}{\delta}G_2^{00} \tag{A24}$$

APPENDIX B: AZIMUTHAL INTEGRALS

$$G_1^{00} = \frac{\pi 2}{\sqrt{(1-\varepsilon^2)}} \tag{B1}$$

$$G_1^{01} = \frac{2\pi\left(1-\sqrt{(1-\varepsilon^2)}\right)}{\varepsilon\sqrt{(1-\varepsilon^2)}} \tag{B2}$$

$$G_1^{02} = 2\pi \frac{1-\sqrt{(1-\varepsilon^2)}}{\varepsilon^2\sqrt{(1-\varepsilon^2)}} \tag{B3}$$

$$G_1^{10} = G_1^{11} = 0 \tag{B4}$$

$$G_1^{20} = \begin{cases} \frac{2\pi\left(1-\sqrt{(1-\varepsilon^2)}\right)}{\varepsilon^2} \text{ if } 0<\varepsilon<1 \\ \pi \text{ if } \varepsilon = 0 \end{cases} \tag{B5}$$

$$G_2^{00} = \frac{2}{\sqrt{(1-\varepsilon^2)^3}}\pi \tag{B6}$$

$$G_2^{01} = 2\pi\frac{\varepsilon}{\sqrt{(1-\varepsilon^2)^3}} \tag{B7}$$

$$G_2^{02} = \begin{cases} \frac{2\pi\left(-1+2\varepsilon^2+\sqrt{(1-\varepsilon^2)^3}\right)}{\varepsilon^2\sqrt{(1-\varepsilon^2)^3}} \text{ if } 0<\varepsilon<1 \\ \pi \text{ if } \varepsilon = 0 \end{cases} \tag{B8}$$

$$G_2^{10} = G_2^{11} = G_2^{30} = 0 \tag{B9}$$

$$G_2^{20} = \begin{cases} \frac{2\pi\left(1-\sqrt{(1-\varepsilon^2)}\right)}{\varepsilon^2\sqrt{(1-\varepsilon^2)}} \text{ if } 0<\varepsilon<1 \\ \pi \text{ if } \varepsilon = 0 \end{cases} \tag{B10}$$

$$G_2^{21} = \frac{-2\pi\left(\varepsilon^2-2+2\sqrt{(1-\varepsilon^2)}\right)}{\varepsilon^3\sqrt{(1-\varepsilon^2)}} \tag{B11}$$

$$G_3^{00} = \begin{cases} \frac{\pi\left(\varepsilon^2+2\right)}{\sqrt{(1-\varepsilon^2)^5}} \text{ if } 0<\varepsilon<1 \\ 2\pi \text{ if } \varepsilon = 0 \end{cases} \tag{B12}$$

$$G_3^{01} = \begin{cases} \frac{\pi 3\varepsilon}{\sqrt{(1-\varepsilon^2)^5}} \text{ if } 0<\varepsilon<1 \\ 0 \text{ if } \varepsilon = 0 \end{cases} \tag{B13}$$

$$G_3^{02} = \begin{cases} \frac{\pi\left(2\varepsilon^2+1\right)}{\sqrt{(1-\varepsilon^2)^5}} \text{ if } 0<\varepsilon<1 \\ \pi \text{ if } \varepsilon = 0 \end{cases} \tag{B14}$$

$$G_3^{10} = G_3^{11} = G_3^{12} = G_3^{30} = 0 \tag{B15}$$

$$G_3^{20} = \begin{cases} \frac{\pi}{\sqrt{(1-\varepsilon^2)^3}} \text{ if } 0<\varepsilon<1 \\ \pi \text{ if } \varepsilon = 0 \end{cases} \tag{B16}$$

$$G_3^{21} = \begin{cases} \frac{-2\pi\left[1-2\varepsilon^2-\left(1+\varepsilon^2\right)\sqrt{(1-\varepsilon^2)}\right]}{\varepsilon^2\sqrt{(1-\varepsilon^2)^3}} \\ \text{if } 0<\varepsilon<1 \\ \\ \pi \text{ if } \varepsilon = 0 \end{cases} \tag{B17}$$

$$G_4^{00} = \frac{\pi\left(3\varepsilon^2+2\right)}{\sqrt{(1-\varepsilon^2)^7}} \tag{B18}$$

$$G_4^{01} = \begin{cases} \frac{\pi\varepsilon\left(\varepsilon^2+4\right)}{\sqrt{(1-\varepsilon^2)^7}} \text{ if } 0<\varepsilon<1 \\ 0 \text{ if } \varepsilon = 0 \end{cases} \tag{B19}$$

$$G_4^{02} = \begin{cases} \frac{\pi\left(4\varepsilon^2+1\right)}{\sqrt{(1-\varepsilon^2)^7}} \text{ if } 0<\varepsilon<1 \\ \pi \text{ if } \varepsilon = 0 \end{cases} \tag{B20}$$

$$G_4^{03} = \begin{cases} \frac{\pi\left(2\varepsilon^2+3\right)\varepsilon}{\sqrt{(1-\varepsilon^2)^7}} \text{ if } 0<\varepsilon<1 \\ 0 \text{ if } \varepsilon = 0 \end{cases} \tag{B21}$$

$$G_4^{04} = \begin{cases} \frac{\pi\left(2-8\varepsilon^6-7\varepsilon^2+8\varepsilon^4+2\left(3\varepsilon^2-3\varepsilon^4+\varepsilon^6-1\right)S\right)}{-\varepsilon^4 S^7} \\ \\ \text{with } S = \sqrt{(1-\varepsilon^2)}, \text{ if } 0<\varepsilon<1 \\ \\ \frac{3}{4}\pi \text{ if } \varepsilon = 0 \end{cases} \tag{B22}$$

$$G_4^{10} = G_4^{11} = G_4^{12} = G_4^{13} = G_4^{30} = 0 \tag{B23}$$

$$G_4^{20} = \begin{cases} \frac{\pi}{\sqrt{(1-\varepsilon^2)^5}} \text{ if } 0<\varepsilon<1 \\ \pi \text{ if } \varepsilon = 0 \end{cases} \tag{B24}$$

$$G_4^{21} = \begin{cases} \frac{\pi\varepsilon}{\sqrt{(1-\varepsilon^2)}(\varepsilon^2-1)^2} \text{ if } 0<\varepsilon<1 \\ 0 \text{ if } \varepsilon = 0 \end{cases} \tag{B25}$$

$$G_4^{22} = \begin{cases} \frac{-\pi\left(5\varepsilon^2-2-4\varepsilon^4+2\left(\varepsilon^2-1\right)^2\sqrt{(1-\varepsilon^2)}\right)}{\varepsilon^4(\varepsilon^2-1)^2\sqrt{(1-\varepsilon^2)}} \\ \text{if } 0<\varepsilon<1 \\ \\ \frac{1}{4}\pi \text{ if } \varepsilon = 0 \end{cases} \tag{B26}$$